JACS
JOURNAL OF THE AMERICAN CHEMICAL SOCIETY

Communication

pubs.acs.org/JACS

Femtosecond Ligand/Core Dynamics of Microwave-Assisted Synthesized Silicon Quantum Dots in Aqueous Solution

Tonya M. Atkins,[†] Arthur Thibert,[†] Delmar S. Larsen,*[,†] Sanchita Dey,[‡] Nigel D. Browning,[‡] and Susan M. Kauzlarich*[,†]

[†]Department of Chemistry and [‡]Department of Chemical Engineering and Materials Science, University of California, Davis, One Shields Avenue, Davis, California 95616, United States

Supporting Information

ABSTRACT: A microwave-assisted reaction has been developed to produce hydrogen-terminated silicon quantum dots (QDs). The Si QDs were passivated for water solubility via two different methods: hydrosilylation produced 3-aminopropenyl-terminated Si QDs, and a modified Stöber process produced silica-encapsulated Si QDs. Both methods produce water-soluble QDs with maximum emission at 414 nm, and after purification, the QDs exhibit intrinsic fluorescence quantum yield efficiencies of 15 and 23%, respectively. Even though the QDs have different surfaces, they exhibit nearly identical absorption and fluorescence spectra. Femtosecond transient absorption spectroscopy was used for temporal resolution of the photoexcited carrier dynamics between the QDs and ligand. The transient dynamics of the 3-aminopropenyl-terminated Si QDs is interpreted as a formation and decay of a charge-transfer (CT) excited state between the delocalized π electrons of the carbon linker and the Si core excitons. This CT state is stable for ~4 ns before reverting back to a more stable, long-living species. The silica-encapsulated Si QDs show a simpler spectrum without CT dynamics.

Silicon quantum dots (QDs) are of great interest for applications in biomedicine, electronics, optoelectronics, nonlinear optics, and solar energy.[1,2] As seen from the variety of possible uses, Si QDs have significant potential, but solution or colloidal synthetic methods remain underdeveloped. Although a variety of high-temperature methods for preparing Si QDs exist (e.g., laser pyrolysis, plasma decomposition, and heat treatment under reducing atmospheres), colloidal chemistry approaches provide the unique opportunity to control the size and surface of the Si QDs simultaneously.[1,3−7] While there has been promising progress in preparing Si QDs in solution, the application of microwave-assisted solution synthesis has not yet been demonstrated. The synthetic method presented herein provides an efficient synthesis of hydrogen-terminated Si QDs without the use of HF. Transient absorption spectroscopy provided insight to the nature of the photocarriers, indicating that with appropriate ligand conjugation, complex photodynamics exist between the ligand environment and the Si QD core, suggesting an energy- or electron-transfer process that can be tuned to optimize the photophysical processes for a variety of applications (e.g., increased fluorescence quantum yield).

During the past two decades, microwave chemistry has been growing as a successful means of controlled synthesis in organic chemistry. While there have been reports of successful microwave-assisted syntheses of II−IV semiconductor QDs,[8−10] this method has not been demonstrated for Si QDs. Microwave-assisted synthesis has advantages such as uniform heating of solvents and localized heating of reactants. Microwave dielectric heating can also accelerate reactions 1000-fold depending on the solvent.[11] Moreover, doped Si has been shown to absorb microwaves efficiently, and microwave irradiation has been demonstrated as an efficient method for passivating porous silicon surfaces with 1-alkenes.[12,13] A simple, rapid, and efficient synthetic route to water-soluble Si QDs would be advantageous for the further development of their use in fields such as molecular biology and biomedical engineering, where the use of air-sensitive reactive precursors may be a significant barrier.

Solution-phase chemistry, either of metal silicides with silicon halides and ammonium halides or via oxidation or reduction routes, has introduced many new pathways for generating organically capped and stable Si nanoparticles.[14−19] One successful example is the reaction of sodium silicide, Na_4Si_4, with ammonium bromide, NH_4Br, performed through standard Schlenk techniques to produce hydrogen-terminated Si nanoparticles.[20] These Si QDs can be produced in a three day period by reflux of the starting reagents followed by isolation and purification. Alkylamine- and acid-terminated Si nanoparticles have also been demonstrated and shown to be water stable for biological imaging applications.[18,21] The use of metal silicides as reactive precursors exhibits additional versatility in generating water-soluble magnetic resonance/optical multimodal probes.[22,23]

A microwave-assisted reaction has been developed to produce hydrogen-terminated Si QDs that are further reacted via hydrosilylation[24] or a modified Stöber process[25] to form photoluminescent Si QDs (Scheme 1). The 3-aminopropenyl-terminated Si QDs were produced by a simple one-pot, two-step microwave-assisted reaction, as illustrated in Scheme 1A. Scheme 1B shows the reaction used to produce the silica-encapsulated Si QDs. The optimal reaction parameters are indicated in Scheme 1. In a typical reaction, Na_4Si_4 and NH_4Br

Received: August 10, 2011
Published: November 22, 2011

   dx.doi.org/10.1021/ja207344u | *J. Am. Chem.Soc.* 2011, 133, 20664−20667

Scheme 1. Microwave-Assisted Syntheses of (A) 3-Aminopropenyl-Terminated and (B) Silica-Encapsulated Si QDs

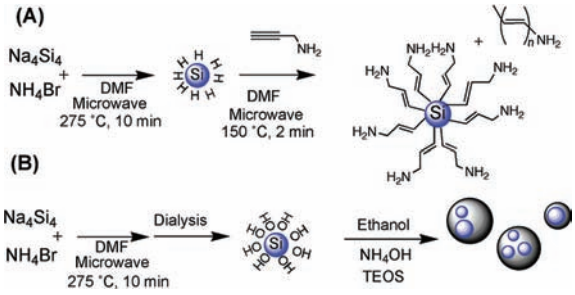

were loaded into a microwave reaction vessel, and *N*,*N*-dimethylformamide (DMF) was added under an inert atmosphere before the reaction vessel was sealed and placed into the microwave reactor. After heat treatment, the reaction vessel was allowed to cool. For the hydrosilylation procedure (Scheme 1A), propargylamine was then added under an inert atmosphere, and the reaction vessel was sealed and placed into the microwave reactor for a second short heating step. The final product was purified via dialysis or chromotography. To obtain silica-encapsulated Si QDs (Scheme 1B), the microwave-synthesized QDs were separated from the salt byproduct via dialysis and transferred to ethanol. The silica shell was then formed by the base-catalyzed reaction of Tetraethoxysilane (TEOS). The silica-encapsulated Si QDs consisted of both multiple Si QDs encased in silica and individual Si QDs with a silica coating (Scheme 1B). A thermal reaction under similar conditions in a pressure vessel resulted in negligible yields, suggesting that the microwave absorption by the rapidly formed Si QDs is important.

A typical transmission electron microscopy (TEM) image and a high-resolution scanning TEM (HRSTEM) image of 3-aminopropenyl-terminated Si QDs produced via Scheme 1A are shown in Figure 1. The average particle diameter was found

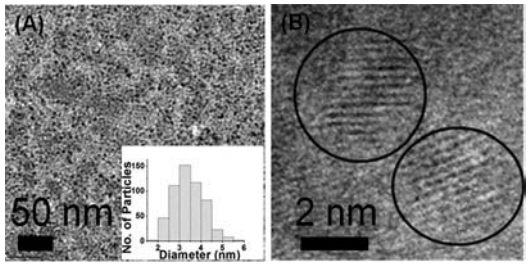

Figure 1. (A) TEM image and (inset) size distribution histogram for 3-aminopropenyl-terminated Si QDs. (B) Bright-field HRSTEM image of the Si QDs showing lattice fringes consistent with the (111) and (220) spacing of diamond-structured silicon.

to be 3.4 ± 0.7 nm, as indicated in the inset histogram. The bright-field HRSTEM image of the 3-aminopropenyl-terminated Si QDs resolved lattice fringes consistent with the (111) spacing of 0.313 nm and the (220) spacing of 0.192 nm for diamond-structured silicon (upper-left and lower-right circles, respectively, in Figure 1B). The TEM images of silica-encapsulated Si QDs synthesized via Scheme 1B (Figure 2) indicate that the Si QDs are completely encapsulated in silica, which imparts water solubility without introducing additional organic moieties.

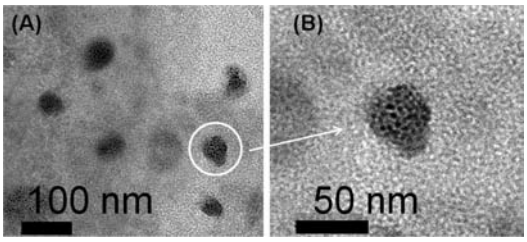

Figure 2. (A) TEM image of silica-encapsulated Si QDs. (B) Higher-magnification image showing that the silica nanoparticles contain small Si nanoparticles.

The absorption and photoluminescence emission spectra of the 3-aminopropenyl-terminated and silica-encapsulated Si QDs are strikingly similar, with the strongest emission in the blue region of visible light (Figure 3). The excitation and

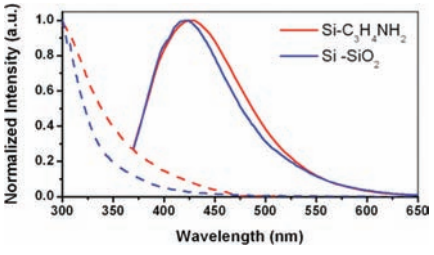

Figure 3. Normalized static emission (solid curves) and absorption spectra (dashed curves) of 3-aminopropenyl-terminated Si QDs (red) and silica-encapsulated (blue) Si QDs in water. The absorption spectra were normalized at 310 nm.

emission spectra are similar to those alkyl- and alkylamine-terminated Si QDs reported in the literature, which are all prepared by solution colloidal routes.[7,17,18,20,23,26] Moreover, the maximum wavelengths for all of the samples produced with the investigated reaction parameters were nearly identical, suggesting that this method generates Si QDs with similar size populations. TEM characterization was consistent with this hypothesis. Longer reaction times at a given temperature did not drive Ostwald ripening to produce larger Si QDs emitting at longer wavelengths. However, it appears for the 20 min reaction time that a slight increase in the number of smaller-sized Si QDs was observed. The general lack of Si QD growth with increasing time was confirmed by TEM characterization, which consistently showed small-diameter Si QDs (3−4 nm). Unlike reduction routes, where the size is correlated with the ratio of precursor to reducing agent, the particle size for this reaction may be limited by the solubility of Na_4Si_4 and/or the concentrations of precursors in solution.[14]

The 3-aminopropenyl-terminated Si QDs exhibit an average fluorescence quantum yield (QY) of ∼15% (average of three different samples) in water after purification, similar to that reported for 3-aminopropyl-terminated Si QDs obtained by thermal methods.[7,27] Typical QYs for alkylamine-capped Si QDs in water have been reported to be 13.2 ± 0.6%.[7] Light emission by nanocrystalline Si has been attributed to both quantum-confinement effects and a reduction in the rate of nonradiative combinations.[28,29] Prior to purification, the particles' QY in water was significantly higher (∼26%). Evidence for the presence of polymer in the unpurified product and the removal of the polymer via dialysis was apparent from both the changes in QY and the TEM images when the

dx.doi.org/10.1021/ja207344u | *J. Am. Chem.Soc.* 2011, 133, 20664−20667

as-prepared product was compared with the purified product [see the Supporting Information (SI)].

In water at neutral pH, the amine groups of the 3-aminopropenyl-terminated Si QDs are protonated. FTIR spectra (see the SI) indicated that while the microwave-assisted hydrosilylation of the Si QDs was successful, the surface of the Si QDs showed oxidation, similar to what is observed for porous Si.[12] The FTIR spectrum (Figure SI2) for the silica-encapsulated Si QDs exhibits both O−H and Si−O−Si stretches along with at least one resonance that might be attributed to the C═O stretch of DMF, suggesting that the surface capping is more complex.

The femtosecond transient absorption signals (see below) indicate that a photoinduced distonic [charge-transfer (CT)] population exists, giving rise to the enhanced QY (26%) of the polymer/Si QD mixture. The polymer is removed via dialysis or chromatography, resulting in a QY of 12−15% for the purified 3-aminopropenyl-termined Si QDs. In the case of the reaction without propargylamine (i.e., for silica-encapsulated QDs; Scheme 1B), a QY of 23.3 ± 0.3% was obtained. The higher QY for the silica-encapsulated sample may result from temperature-localized heating of the sample via microwave absorption along with more efficient passivation of the surface by the inorganic silica shell.

The nearly identical absorption and emission spectra of the 3-aminopropenyl-terminated and silica-encapsulated Si QDs (Figure 3) hindered the characterization and differentiation of the influence of the surface-passivating 3-aminopropenyl ligand and silica environments on the electronic structure and photodynamics, including the fluorescence QYs of the Si QD cores. To unravel this, 400 nm-initiated dispersed ultrafast transient absorption signals were measured and compared. The silica-encapsulated Si QDs signals (Figure 4A) exhibited little

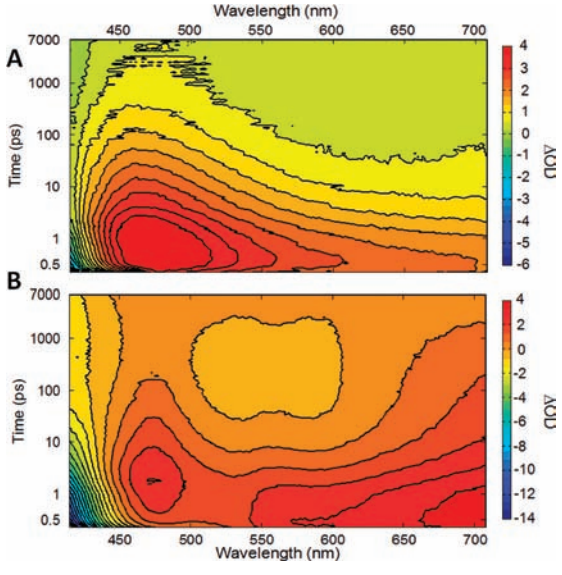

Figure 4. Transient absorption contour plots depicting the spectral evolution of (A) silica-encapsulated and (B) 3-aminopropenyl-terminated Si QDs suspended in H_2O. Data were collected at a flux of 26.5 μJ pulse^{-1} mm^{-2}.

resolvable spectral evolution of a broad, positive induced absorption. Significantly richer dynamics were observed for the 3-aminopropenyl-terminated Si QDs (Figure 4B), which exhibited a structure-induced absorption that evolved into a negative signal from 500 to 600 ns within 100 ps (this is better seen in the kinetic traces in Figure SI6).

These data were modeled using global analysis to estimate evolutionary associated difference spectra (EADS) with the associated concentration profiles of the underlying dynamic populations (Figure 5):[30]

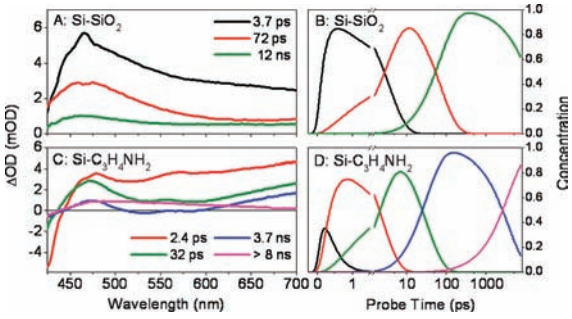

Figure 5. (A, C) Global analysis EADS extracted from (A) a three-compartment sequential global analysis fitting scheme associated with silica-encapsulated Si QDs and (C) a five-compartment scheme associated with 3-aminopropenyl-terminated Si QDs. (B, D) Concentration profiles of the corresponding populations. The data for the 220 fs population for the 3-aminopropenyl-terminated Si QDs are not shown in (A) and (B) to aid in interpretation; they are displayed in Figure SI5.

$$\frac{dn_i}{dt} = A_i I(t) + \sum_j K_{ij} n_j \quad (1)$$

where n_i represents the population of interest, $A_i I(t)$ is the correlation of the 125 fs pump pulse duration with the initial distribution of excitation used to describe the rise, and K_{ij} is the rate constant matrix describing the flow of population from one compartment into another. Only three compartments were required for a full description of the data for the silica-encapsulated Si QDs (3.7 ps, 72 ps, and ∼12 ns) (Figure 5A,B), and the induced absorption is ascribed to trapped charges on the basis of the observed relaxation time constants.[31,32] Similar kinetics and spectra were observed in the dynamics of octene-capped Si QDs, demonstrating that the SiO_2 passivates surface traps of the Si QDs equally well as long-chain alkanes.[31] The faster decay kinetics (72 ps) observed on the blue edge versus the red edge (12 ns) is a signature of excited-state inhomogeneity and is similar to the photoluminescence signals resolved in alkane-terminated Si QDs by Klimov et al.[33] that were ascribed to core- and surface-trapped excitations, respectively.

Five characteristic populations (200 fs, 2.4 ps, 32 ps, 3.7 ns, and >8 ns) were needed to describe the data for the 3-aminopropenyl-terminated Si QDs with EADS extending across the entire spectral and temporal windows. The initial spectrum was largely positive (red curves in Figure 5C,D) and decayed on a 2.4−32 ps time scale into populations with a clear stimulated emission (SE) contribution peaking at 535 nm and overlapping a broad, positive induced absorption signal. This population persisted for ∼4 ns before reverting to a stable, long-living species (magenta curves in Figure 5C,D) that qualitatively resembles the species producing the final spectrum for the silica-encapsulated Si QDs (green curve in Figure 5A). The populations responsible for the SE closely resemble the spectra for transient emissive populations in organic molecules, suggesting that the 3-aminopropenyl ligand is excited in the sample.

dx.doi.org/10.1021/ja207344u | J. Am. Chem.Soc. 2011, 133, 20664−20667

However, since the energy of the HOMO−LUMO gap for isolated 3-aminopropenyl ligands is ≥330 nm (based on the UV−vis spectrum in Figure SI4), direct excitation of the ligand with the ultrafast 400 nm pulses is negligible. Consequently, excitation of the 3-aminopropenyl ligand (via the observed SE signals) primarily results from the interactions (e.g., charge- or energy-transfer) with photoexcited Si excitons. We propose that an electron- or hole-transfer reaction (possibly involving the lone pair on the amine N) occurs, facilitated by conjugation from the Si QD through the C═C double bond (Scheme 1A). Vertical excitation of the Si QD core with 400 nm light induces rapid CT (likely between the lone-pair electrons of the $-NH_2$ or $-NH_3^+$ groups on the 3-aminopropenyl ligand and the Si core) to generate a metastable CT state. This state persists for 3.7 ns before back-CT occurs, forming a stabilized localized excited state (Figure 5, magenta curves). It is unclear whether the CT state is formed from electron transfer from the core to the ligand or from the ligand to the core, although the latter is more likely given the high reduction potential of $-NH_2$.

This mechanism is different from that observed by Kryschi and co-workers,[32] who recently proposed a photoinitiated charge- or electron-transfer mechanism from direct photoexcitation of the 3-vinylthiophene ligands capping the Si QDs via high-energy two-photon excitation. The signals presented above are one-photon-initiated with a linear dependence on excitation power.

The microwave-assisted synthesis of Si QDs has been demonstrated to be easily performed, efficient, and reproducible. Highly photoluminescent Si QDs can be obtained in as little as 12 min, as opposed to several days in typical thermal reactions. In this study, hydrosilylation and a modified Stöber method have been investigated, and this microwave-assisted synthesis can be further expanded to other ligands and capping agents. Microwave-assisted heating produced Si QDs with QYs in water as high as 23%. Femtosecond transient absorption spectroscopy could temporally resolve the photoexcited carrier dynamics between the QDs and ligand. The transient dynamics of the 3-aminopropenyl-terminated Si QDs are interpreted as an admixture of the silica-encapsulated Si QDs dynamics with an excited-state CT process between the delocalized π electrons of the carbon linker and the Si core excitons. The silica-encapsulated Si QDs show a simpler spectrum without CT dynamics. These results suggest that the CT process may be tuned to optimize the photodynamic processes. The ability to produce electronic coupling in nanomaterials has potential applications in the design of new multicomponent systems with desired CT properties and opens up new opportunities in optoelectronic applications.

■ ASSOCIATED CONTENT

Supporting Information

Detailed synthesis protocols, experimental methods, and additional transient data. This material is available free of charge via the Internet at http://pubs.acs.org.

■ AUTHOR INFORMATION

Corresponding Author

dlarsen@ucdavis.edu; smkauzlarich@ucdavis.edu

■ ACKNOWLEDGMENTS

This research was supported by DOE (DESC0002289) and NSF (DMR-1035468). We thank Angelique Louie for useful discussions. The high-resolution microscopy experiments were supported by the U.S. Department of Energy, Office of Basic Energy Sciences, Division of Materials Sciences and Engineering, under Grant DE-FG0203ER46057.

■ REFERENCES

(1) Kortshagen, U. *J. Phys. D: Appl. Phys.* **2009**, *42*, No. 113001.
(2) Veinot, J. G. C. *Chem. Commun.* **2006**, 4160.
(3) Anthony, R.; Kortshagen, U. *Phys. Rev. B* **2009**, *80*, No. 115407.
(4) Holmes, J. D.; Ziegler, K. J.; Doty, R. C.; Pell, L. E.; Johnston, K. P.; Korgel, B. A. *J. Am. Chem. Soc.* **2001**, *123*, 3743.
(5) Li, X. G.; He, Y. Q.; Talukdar, S. S.; Swihart, M. T. *Langmuir* **2003**, *19*, 8490.
(6) Tilley, R. D.; Yamamoto, K. *Adv. Mater.* **2006**, *18*, 2053.
(7) Rosso-Vasic, M.; Spruijt, E.; Popovic, Z.; Overgaag, K.; van Lagen, B.; Grandidier, B.; Vanmaekelbergh, D.; Dominguez-Gutierrez, D.; De Cola, L.; Zuilhof, H. *J. Mater. Chem.* **2009**, *19*, 5926.
(8) Gerbec, J. A.; Magana, D.; Washington, A.; Strouse, G. F. *J. Am. Chem. Soc.* **2005**, *127*, 15791.
(9) Washington, A. L.; Strouse, G. F. *Chem. Mater.* **2009**, *21*, 3586.
(10) Zhu, M. Q.; Gu, Z.; Fan, J. B.; Xu, X. B.; Cui, J.; Liu, J. H.; Long, F. *Langmuir* **2009**, *25*, 10189.
(11) Gabriel, C.; Gabriel, S.; Grant, E. H.; Halstead, B. S. J.; Mingos, D. M. P. *Chem. Soc. Rev.* **1998**, *27*, 213.
(12) Boukherroub, R.; Petit, A.; Loupy, A.; Chazalviel, J.-N.; Ozanam, F. *J. Phys. Chem. B* **2003**, *107*, 13459.
(13) Petit, A.; Delmotte, M.; Loupy, A.; Chazalviel, J.-N.; Ozanam, F.; Boukherroub, R. *J. Phys. Chem. C* **2008**, *112*, 16622.
(14) Zou, J.; Sanelle, P.; Pettigrew, K. A.; Kauzlarich, S. M. *J. Cluster Sci.* **2006**, *17*, 565.
(15) Zou, J.; Kauzlarich, S. M. *J. Cluster Sci.* **2008**, *19*, 341.
(16) Zou, J.; Baldwin, R. K.; Pettigrew, K. A.; Kauzlarich, S. M. *Nano Lett.* **2004**, *4*, 1181.
(17) Pettigrew, K. A.; Liu, Q.; Power, P. P.; Kauzlarich, S. M. *Chem. Mater.* **2003**, *15*, 4005.
(18) Zhang, X. M.; Neiner, D.; Wang, S. Z.; Louie, A. Y.; Kauzlarich, S. M. *Nanotechnology* **2007**, *18*, No. 095601.
(19) Bley, R. A.; Kauzlarich, S. M. *J. Am. Chem. Soc.* **1996**, *118*, 12461.
(20) Neiner, D.; Chiu, H. W.; Kauzlarich, S. M. *J. Am. Chem. Soc.* **2006**, *128*, 11016.
(21) Manhat, B. A.; Brown, A. L.; Black, L. A.; Ross, J. B. A.; Fichter, K.; Vu, T.; Richman, E.; Goforth, A. M. *Chem. Mater.* **2011**, *23*, 2407.
(22) Tu, C. Q.; Ma, X. C.; Pantazis, P.; Kauzlarich, S. M.; Louie, A. Y. *J. Am. Chem. Soc.* **2010**, *132*, 2016.
(23) Tu, C. Q.; Ma, X. C.; House, A.; Kauzlarich, S. M.; Louie, A. Y. *ACS Med. Chem. Lett.* **2011**, *2*, 285.
(24) Buriak, J. M. *Chem. Rev.* **2002**, *102*, 1271.
(25) Stöber, W.; Fink, A.; Bohn, E. J. *J. Colloid Interface Sci.* **1968**, *26*, 62.
(26) Warner, J. H.; Rubinsztein-Dunlop, H.; Tilley, R. D. *J. Phys. Chem. B* **2005**, *109*, 19064.
(27) Warner, J. H.; Hoshino, A.; Yamamoto, K.; Tilley, R. D. *Angew. Chem., Int. Ed.* **2005**, *44*, 4550.
(28) Delerue, C.; Allan, G.; Lannoo, M. *Phys. Rev. B* **2001**, *64*, No. 193402.
(29) Brus, L. E.; Szajowski, P. F.; Wilson, W. L.; Harris, T. D.; Schuppler, S.; Citrin, P. H. *J. Am. Chem. Soc.* **1995**, *117*, 2915.
(30) van Stokkum, I. H. M.; Larsen, D. S.; van Grondelle, R. *Biochim. Biophys. Acta* **2004**, *1657*, 82.
(31) Zhang, X.; Brynda, M.; Britt, R. D.; Carroll, E. C.; Larsen, D. S.; Louie, A. Y.; Kauzlarich, S. M. *J. Am. Chem. Soc.* **2007**, *129*, 10668.
(32) Groenewegen, V.; Kuntermann, V.; Haarer, D.; Kuntz, M.; Kryschi, C. *J. Phys. Chem. C* **2010**, *114*, 11693.
(33) Sykora, M.; Mangolini, L.; Schaller, R. D.; Kortshagen, U.; Jurbergs, D.; Klimov, V. I. *Phys. Rev. Lett.* **2008**, *100*, No. 067401.